International Journal of Bridge Engineering (IJBE), Vol. 6, No. 3, (2018), pp. 19-44

BIAXIAL BUCKLING OF THIN LAMINATED COMPOSITE PLATES

Osama Mohammed Elmardi Suleiman Khayal [1],
Mahmoud Yassin Osman[2] and Tagelsir Hassan[3]

[1,2] Nile Valley University, Dept. of Mechanical Engineering, Sudan
[3] Omdurman Islamic University, Dept. of Mechanical Engineering, Sudan
e-mail: osamamm64@gmail.com, osman.maya@gmail.com, tagelsirhussan@hotmail.co.uk

ABSTRACT: Finite element (FE) method is presented for the analysis of thin rectangular laminated composite plates under the biaxial action of in – plane compressive loading, such plates are common on bridges. The analysis uses the classical laminated plate theory (CLPT) which does not account for shear deformations. In this theory it is assumed that the laminate is in a state of plane stress, the individual lamina is linearly elastic, and there is perfect bonding between layers. The classical laminated plate theory (CLPT), which is an extension of the classical plate theory (CPT) assumes that normal to the mid – surface before deformation remains straight and normal to the mid – surface after deformation. Therefore, this theory is only adequate for buckling analysis of thin laminates.

A Fortran program has been compiled. New numerical results are generated for in – plane compressive biaxial buckling which serve to quantify the effects of lamination scheme, aspect ratio, material anisotropy, fiber orientation of layers, reversed lamination scheme and boundary conditions.

It was found that symmetric laminates are stiffer than the anti – symmetric one due to coupling between bending and stretching which decreases the buckling loads of symmetric laminates. The buckling load increases with increasing aspect ratio, and decreases with increase in modulus ratio. The buckling load will remain the same even when the lamination order is reversed. The buckling load increases with the mode number but at different rates depending on the type of end support. It is also observed that as the mode number increases, the plate needs additional support.

KEYWORDS: Finite element method; classical plate theory; buckling; thin plates; laminated composites; new numerical results.

1 INTRODUCTION

Composites were first considered as structural materials a little more than three quarters of a century ago. From that time to now, they have received increasing

attention in all aspects of material science, manufacturing technology, and theoretical analysis, such plates are common on bridges.

The term composite could mean almost anything if taken at face value, since all materials are composites of dissimilar subunits if examined at close enough details. But in modern materials engineering, the term usually refers to a matrix material that is reinforced with fibers. For instance, the term "FRP" which refers to Fiber Reinforced Plastic usually indicates a thermosetting polyester matrix containing glass fibers, and this particular composite has the lion's share of today commercial market.

Many composites used today are at the leading edge of materials technology, with performance and costs appropriate to ultra-demanding applications such as space crafts. But heterogeneous materials combining the best aspects of dissimilar constituents have been used by nature for millions of years. Ancient societies, imitating nature, used this approach as well: The book of Exodus speaks of using straw to reinforce mud in brick making, without which the bricks would have almost no strength. Here in Sudan, people from ancient times dated back to Meroe civilization, and up to now used zibala (i.e. animals' dung) mixed with mud as a strong building material.

As seen in table 1 below, which is cited by David Roylance [1], Stephen et al. [2], Turvey et al. [3], and Mahmoud Yassin Osman and Osama Mohammed Elmardi [4], [5], [6] and [7], the fibers used in modern composites have strengths and stiffnesses far above those of traditional structural materials. The high strengths of the glass fibers are due to processing that avoids the internal or external textures flaws which normally weaken glass, and the strength and stiffness of polymeric aramid fiber is a consequence of the nearly perfect alignment of the molecular chains with the fiber axis.

Table 1. Properties of composite reinforcing fibers

Material	E (GN/m^2)	σ_b (GN/m^2)	ε_b (%)	ρ (Mg/m^3)	E/ρ (MN.m/kg)	σ_b/ρ (MN.m/kg)
E-glass	72.4	2.4	2.6	2.54	28.5	0.95
S-glass	85.5	4.5	2.0	2.49	34.3	1.8
Aramid	124	3.6	2.3	1.45	86	2.5
Boron	400	3.5	1.0	2.45	163	1.43
H S graphite	253	4.5	1.1	1.80	140	2.5
H M graphite	520	2.4	0.6	1.85	281	1.3

Where E is Young's modulus, σ_b is the breaking stress, ε_b is the breaking strain, and ρ is the mass density.

The theory used in the present work comes under the class of displacement-based theories. Extensions of these theories which include the linear terms in z

in u and v and only the constant term in w, to account for higher – order variations and to laminated plates, can be found in the work of Yang, Norris and Stavsky [8], Whitney and Pagano [9], Phan and Reddy [10] and Mahmoud Yassin Osman and Osama Mohammed Elmardi [11]. In the present work, classical plate theory is used, which is appropriate for thin laminated plates.
In the present study, the composite media are assumed free of imperfections i.e. initial geometrical imperfections due to initial distortion of the structure, and material and / or constructional imperfections such as broken fibers, delaminated regions, cracks in the matrix material, foreign inclusions and small voids which are due to inconvenient selection of fibers / matrix materials and manufacturing defects. Therefore, the fibers and matrix are assumed perfectly bonded.

2 MATHEMATICAL FORMULATIONS

Consider a thin plate of length a, breadth b, and thickness h as shown in Figure 1(a), subjected to in – plane loads R_x , R_y and R_{xy} as shown in Figure 1(b). The in – plane displacements $u(x, y, z)$ and $v(x, y, z)$, can be expressed in terms of the out – of – plane displacement $w(x, y)$ as shown below.

$$u = -z\frac{\partial w}{\partial x} \qquad (1)$$

$$v = -z\frac{\partial w}{\partial y}$$

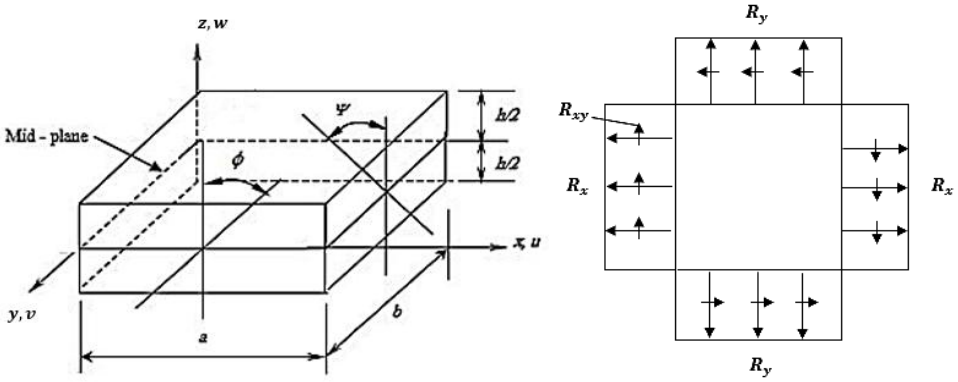

(a) (b)

Figure 1

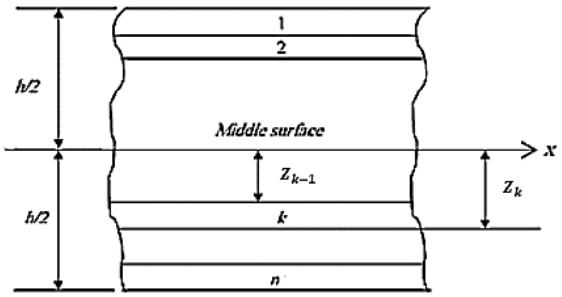

Figure 2. Geometry of an n-Layered laminate

The plate shown in figure 1(a) is constructed of an arbitrary number of orthotropic layers bonded together as in figure 2 above. The strain – displacement relations according to the large deformation theory are:

$$\epsilon_x = \frac{\partial u}{\partial x} + \frac{1}{2}\left(\frac{\partial w}{\partial x}\right)^2 = -z\frac{\partial^2 w}{\partial x^2} + \frac{1}{2}\left(\frac{\partial w}{\partial x}\right)^2$$

$$\epsilon_y = \frac{\partial v}{\partial y} + \frac{1}{2}\left(\frac{\partial w}{\partial y}\right)^2 = -z\frac{\partial^2 w}{\partial y^2} + \frac{1}{2}\left(\frac{\partial w}{\partial y}\right)^2$$

$$\epsilon_{xy} = \frac{\partial v}{\partial x} + \frac{\partial u}{\partial y} + \frac{\partial w}{\partial x}\frac{\partial w}{\partial y} = -2z\frac{\partial^2 w}{\partial x\,\partial y} + \frac{\partial w}{\partial x}\frac{\partial w}{\partial y}$$

These can be written as:

$$\epsilon = \epsilon_1 + \epsilon_2$$

Where, $\epsilon = [\epsilon_x\ \epsilon_y\ \epsilon_{xy}]^T$ and ϵ_1 and ϵ_2 represent the linear and non – linear parts of the strain, i.e.

$$\epsilon_1 = -z\left[\frac{\partial^2 w}{\partial x^2}\quad \frac{\partial^2 w}{\partial y^2}\quad 2\frac{\partial w}{\partial x\,\partial y}\right]^T \tag{2}$$

$$\epsilon_2 = \frac{1}{2}\left[\left(\frac{\partial w}{\partial x}\right)^2\ \left(\frac{\partial w}{\partial y}\right)^2\ 2\frac{\partial w}{\partial x}\frac{\partial w}{\partial y}\right]^T \tag{3}$$

The virtual linear strains can be written as:

$$\delta\epsilon_1 = -z\left[\frac{\partial^2}{\partial x^2}\quad \frac{\partial^2}{\partial y^2}\quad 2\frac{\partial^2}{\partial x\,\partial y}\right]^T \delta w \tag{4}$$

The virtual linear strains energy

$$\delta U = \int_V \delta\epsilon_1^T \sigma\, dV \tag{5}$$

Where V denotes volume
The stress – strain relations,

$$\sigma = \mathrm{C}\,\epsilon_1$$

Where C are the material properties.

$$\mathrm{C} = \begin{bmatrix} \mathrm{C}_{11} & \mathrm{C}_{12} & \mathrm{C}_{16} \\ \mathrm{C}_{12} & \mathrm{C}_{22} & \mathrm{C}_{26} \\ \mathrm{C}_{16} & \mathrm{C}_{26} & \mathrm{C}_{66} \end{bmatrix}$$

Where $\mathrm{C_{ij}}$ are given in Appendix (A).
Substitute for σ in equation (5).

$$\delta\,\mathrm{U} = \int_{\mathrm{V}} \delta\epsilon_1^{\mathrm{T}}\mathrm{C}\,\epsilon_1^{\mathrm{T}}\mathrm{dV} \tag{6}$$

Now express w in terms of the shape functions N (given in Appendix (B)) and nodal displacements $\mathrm{a^e}$, equation (2) can be written as:

$$\delta\,\epsilon_1 = -\mathrm{z}\,\mathrm{B}\,\delta\,\mathrm{a^e}$$

Where,

$$B_i = \left[\frac{\partial^2 N_i}{\partial\, x^2} \quad \frac{\partial^2 N_i}{\partial\, y^2} \quad 2\frac{\partial^2 N_i}{\partial x\, \partial y}\right]^T$$

Hence equation (6) can be written in the form,

$$\delta\, U = \int_V (B\ \delta\ a^e)^T (C\ z^2)\,(B\ a^e)\ dV$$

or

$$\delta\,\mathrm{U} = \delta\,\mathrm{a^{e^T}} \int \mathrm{B^T D\ B\ a^e}\ \mathrm{dx\ dy}$$

Where,

$$\mathrm{D} = \sum_{\mathrm{k=1}}^{\mathrm{n}} \int_{\mathrm{z_{k-1}}}^{\mathrm{z_k}} \mathrm{C\,z^2\ dz}$$

Hence, the virtual strain energy,

$$\delta\,\mathrm{U} = \delta\,\mathrm{a^{e^T} K^e\ a^e} \tag{7}$$

Where $\mathrm{K^e}$ is the element stiffness matrix,

$$\text{i. e.} \qquad \mathrm{K^e} = \int \mathrm{B^T D\ B\ dx\ dy} \tag{8}$$

Now equation (3) can be written in the form,

$$\epsilon_2 = \frac{1}{2}\begin{bmatrix} \dfrac{\partial\,\mathrm{w}}{\partial\,\mathrm{x}} & 0 \\ 0 & \dfrac{\partial\,\mathrm{w}}{\partial\,\mathrm{y}} \\ \dfrac{\partial\,\mathrm{w}}{\partial\,\mathrm{y}} & \dfrac{\partial\,\mathrm{w}}{\partial\,\mathrm{x}} \end{bmatrix} \begin{bmatrix} \dfrac{\partial\,\mathrm{w}}{\partial\,\mathrm{x}} \\ \dfrac{\partial\,\mathrm{w}}{\partial\,\mathrm{y}} \end{bmatrix}$$

The non – linear virtual strain,

$$\delta\,\epsilon_2 = \begin{bmatrix} \frac{\partial}{\partial x}\delta w & 0 \\ 0 & \frac{\partial}{\partial y}\delta w \\ \frac{\partial}{\partial y}\delta w & \frac{\partial}{\partial x}\delta w \end{bmatrix} \begin{bmatrix} \frac{\partial w}{\partial x} \\ \frac{\partial w}{\partial y} \end{bmatrix}$$

The virtual work,

$$\delta W = \int_V \delta\epsilon_2^T \sigma\, dV = \int_V \begin{bmatrix} \frac{\partial w}{\partial x} & \frac{\partial w}{\partial y} \end{bmatrix} \begin{bmatrix} \frac{\partial}{\partial x}\delta w & 0 & \frac{\partial}{\partial y}\delta w \\ 0 & \frac{\partial}{\partial y}\delta w & \frac{\partial}{\partial x}\delta w \end{bmatrix} \begin{bmatrix} \sigma_x \\ \sigma_y \\ \sigma_{xy} \end{bmatrix} dV$$

$$\delta W = \int \begin{bmatrix} \frac{\partial w}{\partial x} & \frac{\partial w}{\partial y} \end{bmatrix} \begin{bmatrix} \frac{\partial}{\partial x}\delta w & 0 & \frac{\partial}{\partial y}\delta w \\ 0 & \frac{\partial}{\partial y}\delta w & \frac{\partial}{\partial x}\delta w \end{bmatrix} \begin{bmatrix} R_x \\ R_y \\ R_{xy} \end{bmatrix} dx\, dy$$

Where,

$$[R_x, R_y, R_{xy}] = \int_{-h/2}^{h/2} [\sigma_x, \sigma_y, \sigma_{xy}]\, dz$$

And σ_x , σ_y , and σ_{xy} are the in – plane stresses.
The previous equation can be written as:

$$\delta W = \int \begin{bmatrix} \frac{\partial}{\partial x}\delta w & \frac{\partial}{\partial y}\delta w \end{bmatrix} \begin{bmatrix} R_x & R_{xy} \\ R_{xy} & R_y \end{bmatrix} \begin{bmatrix} \frac{\partial w}{\partial x} \\ \frac{\partial w}{\partial y} \end{bmatrix} dx\, dy$$

Introducing the shape functions and nodal displacements, we get:

$$\delta W = \delta a^{e\,T} \int \begin{bmatrix} \frac{\partial N_i}{\partial x} & \frac{\partial N_i}{\partial y} \end{bmatrix} \begin{bmatrix} R_x & R_{xy} \\ R_{xy} & R_y \end{bmatrix} \begin{bmatrix} \frac{\partial N_j}{\partial x} \\ \frac{\partial N_j}{\partial y} \end{bmatrix} a^e dx\, dy$$

Now, let $R_x = -P_x$, $R_y = -P_y$, and $R_{xy} = -P_{xy}$

$$\delta W = -\delta a^{e^T} P_x K^{eD} a^e \qquad (9)$$

Where,

$$K^{eD} = \int \left[\frac{\partial N_i}{\partial x} \quad \frac{\partial N_i}{\partial y}\right] \begin{bmatrix} 1 & \frac{P_{xy}}{P_x} \\ \frac{P_{xy}}{P_x} & \frac{P_y}{P_x} \end{bmatrix} \begin{bmatrix} \frac{\partial N_j}{\partial x} \\ \frac{\partial N_j}{\partial y} \end{bmatrix} dx\, dy \qquad (10)$$

K^{eD} is the element differential matrix.
Now,

$$\delta U + \delta W = 0$$

i. e. $$\delta a^{e^T} K^e a^e - \delta a^{e^T} P_x K^{eD} a^e = 0$$

Now since δa^{e^T} is arbitrary and cannot be equal to zero, it follows that,

$$[K^e - P_x K^{eD}]a^e = 0$$

When the plate is divided into a number of elements, the global equation is:

$$[K - P_x K^D]a = 0 \qquad (11)$$

Where,

$$K = \sum K^e, \quad K^D = \sum K^{eD}, a = \sum a^e$$

Since, $a \neq 0$, then the determinant,

$$\left|K - P_x K^D\right| = 0 \qquad (12)$$

Hence, the buckling loads P_x and the buckling modes can be evaluated.
The elements of the stiffness matrix are obtained from equation (8) which can be expanded as follows:

$$K_{ij}^e = \int \left[\frac{\partial^2 N_i}{\partial x^2} \quad \frac{\partial^2 N_i}{\partial y^2} \quad 2\frac{\partial^2 N_i}{\partial x\, \partial y}\right] \begin{bmatrix} D_{11} & D_{12} & D_{16} \\ D_{12} & D_{22} & D_{26} \\ D_{16} & D_{26} & D_{66} \end{bmatrix} \begin{bmatrix} \frac{\partial^2 N_j}{\partial x^2} \\ \frac{\partial^2 N_j}{\partial y^2} \\ 2\frac{\partial^2 N_j}{\partial x\, \partial y} \end{bmatrix} dx\, dy$$

i.e.

$$K_{ij}^e = \int \left[D_{11}\frac{\partial^2 N_i}{\partial x^2}\ \frac{\partial^2 N_j}{\partial x^2} + D_{12}\left(\frac{\partial^2 N_i}{\partial y^2}\frac{\partial^2 N_j}{\partial x^2} + \frac{\partial^2 N_i}{\partial x^2}\frac{\partial^2 N_j}{\partial y^2}\right)\right.$$
$$+D_{22}\frac{\partial^2 N_i}{\partial y^2}\frac{\partial^2 N_j}{\partial y^2} + 4D_{66}\frac{\partial^2 N_i}{\partial x\, \partial y}\frac{\partial^2 N_i}{\partial x\, \partial y} + 2D_{16}\left(\frac{\partial^2 N_i}{\partial x\, \partial y}\frac{\partial^2 N_j}{\partial x^2} + \frac{\partial^2 N_i}{\partial x^2}\frac{\partial^2 N_j}{\partial x\, \partial y}\right)$$
$$\left. +2D_{26}\left(\frac{\partial^2 N_i}{\partial x\, \partial y}\frac{\partial^2 N_j}{\partial y^2} + \frac{\partial^2 N_i}{\partial y^2}\frac{\partial^2 N_j}{\partial x\, \partial y}\right)\right] dxdy \qquad (13)$$

The elements of the differential matrix are obtained from equation (10) which when expanded becomes:

$$K_{ij}^{eD} = \int \left[\frac{\partial N_i}{\partial x} \frac{\partial N_j}{\partial x} + \frac{P_{xy}}{P_x} \left(\frac{\partial N_i}{\partial y} \frac{\partial N_j}{\partial x} + \frac{\partial N_i}{\partial x} \frac{\partial N_j}{\partial y} \right) + \frac{P_y}{P_x} \frac{\partial N_i}{\partial y} \frac{\partial N_j}{\partial y} \right] dx\, dy \quad (14)$$

The integrals in equations (13) and (14) are given in Appendix (C). We use a 4 – noded element as shown in Figure 3 below.

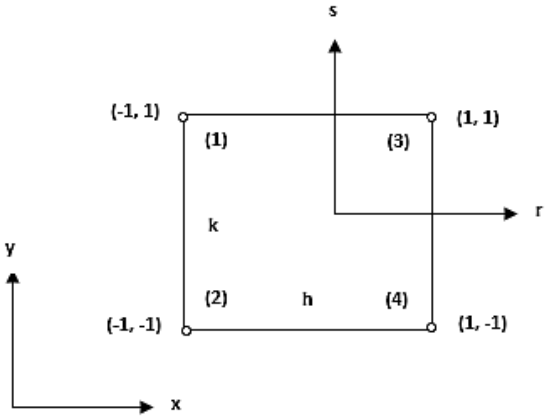

Figure 3

The shape functions for the 4–noded element expressed in global coordinates(x, y). we take:

$$w = N_1 w_1 + N_2 \phi_1 + N_3 \psi_1 + N_4 w_2 + N_5 \phi_2 + N_6 \psi_2$$
$$+ N_7 w_3 + N_8 \phi_3 + N_9 \psi_3 + N_{10} w_4 + N_{11} \phi_4 + N_{12} \psi_4$$

$$\text{where,} \qquad \phi = \frac{\partial w}{\partial x}, \qquad \text{and} \quad \psi = \frac{\partial w}{\partial y}$$

The shape functions in local coordinates (r, s) are as follows:

$$N_i = a_{i,1} + a_{i,2} r + a_{i,3} s + a_{i,4} r^2 + a_{i,5} rs + a_{i,6} s^2 + a_{i,7} r^3$$
$$+ a_{i,8} r^2 s + a_{i,9} rs^2 + a_{i,10} s^3 + a_{i,11} r^3 s + a_{i,12} rs^3$$

Where , $i = 1, 2, 3, \ldots, 12$
The coefficients $a_{i,1}, a_{i,2}, \text{etc}$ are given in Appendix (B).
In the analysis, the following non – dimensional quantities are used:

$$\bar{w} = \left(\frac{1}{h}\right) w , \qquad \bar{\phi} = \left(\frac{h}{a}\right) \phi , \quad \bar{\psi} = \left(\frac{h}{a}\right) \psi$$

$$\bar{D} = \left(\frac{1}{E_1 h^3}\right) D , \qquad \bar{P} = \left(\frac{a^2}{E_1 h^3}\right) P , \quad \bar{b} = b/a$$

Where, E_1 is the modulus in direction of the fiber.

3 BOUNDARY CONDITIONS

All of the analyses described in the present paper have been undertaken assuming the plate to be subjected to identical and/ or different support conditions on the four edges of the plate. The three sets of the of the edge conditions used here are designated as clamped – clamped (CC), simply – simply supported (SS), clamped – simply supported (CS), are shown in table 2 below.

Table 2. Boundary conditions

Boundary Conditions	Plate dimensions in y – coordinate $x = 0 , x = a$	Plate dimensions in x – coordinate $y = 0 , y = b$
CC	$w = \phi = \psi = 0$	$w = \phi = \psi = 0$
SS	$w = \psi = 0$	$w = \phi = 0$
CS	$w = \phi = \psi = 0$	$w = \phi = 0$

4 NUMERICAL RESULTS

With confidence in the finite element (FE) program proved through the various verification exercises undertaken, it was decided to undertake some study cases and generate new results for biaxial loaded laminated composite rectangular plates. The plates were assumed to be simply supported (SS), clamped (CC) and clamped – simply supported (CS) on all four edges.

The problem of critical buckling loads of laminated composite plates is analyzed and solved using the energy method which is formulated by a finite element model. In that model, a four noded rectangular elements of a plate is considered. Each element has three degrees of freedom at each node. The degrees of freedom are the lateral displacement w, and the rotations ϕ and ψ about the y and x axes respectively.

The effects of lamination scheme, aspect ratio, material anisotropy, fiber orientation of layers, reversed lamination scheme and boundary conditions on the non – dimensional critical buckling loads of laminated composite plates are investigated.

The material chosen has the following properties:

$$E_1/E_2 = 5, 10, 20, 25, 40 \; ; \; G_{12} = G_{13} = G_{23} = 0.5E_2 \; ; \; \nu_{12} = 0.25$$

4.1 Effect of lamination scheme

In the present analysis the lamination scheme of plates is supposed to be symmetric, anti – symmetric and quasi – isotropic.

Four lamination schemes were considered which are symmetric and anti – symmetric cross – ply and angle – ply laminates. Table 3 gives a comparison between the non – dimensional buckling loads for all lamination schemes. The results are shown graphically in figure 4. The thickness of all layers is assumed equal, the length to thickness ratio ($a/h = 20$), and the modulus ratio ($E_1/E_2 = 5$). It is noticed from table 3 and figures 4, 5 and 6 that the values of the non –

dimensional buckling loads for both symmetric and anti – symmetric lamination are slightly different, except for symmetric and anti – symmetric angle – ply laminates which are exactly the same. Because of this fact, the rest of the upcoming effects will be discussed for symmetric case only. The results indicate that the symmetric laminate is stiffer than the anti – symmetric one. This phenomenon is caused by coupling between bending and stretching which lowers the buckling loads of symmetric laminate.

Table 3. The first five non – dimensional buckling loads $\bar{P} = Pa^2/E_1h^3$ of symmetric cross – ply (0/ 90/ 90/ 0) and anti – symmetric cross – ply (0/ 90/ 0/ 90), and symmetric angle – ply (45/ -45/ -45/ 45) and anti – symmetric angle – ply (45/ -45/ 45/ -45) laminated plates with $a/h = 20$, and $E_1/E_2 = 5$

Lamination Scheme	Mode Number	Boundary Conditions		
		SS	CC	CS
0/ 90/ 90/ 0	1	0.6972	2.1994	1.8225
	2	1.2522	2.5842	2.0097
	3	2.4284	4.1609	2.7116
	4	2.6907	4.7431	4.3034
	5	2.7346	5.0168	4.4536
0/ 90/ 0/ 90	1	0.6973	2.2273	1.5591
	2	1.9947	3.9687	2.3391
	3	1.9958	3.9732	3.7581
	4	2.6912	4.7871	3.8290
	5	4.3962	7.0544	4.5402
45/-45/-45/45	1	0.8729	1.9505	1.4756
	2	1.6400	2.8534	2.1162
	3	2.3130	3.8941	3.3039
	4	2.7100	4.3753	3.3068
	5	3.5488	5.2694	4.4166
45/-45/45/-45	1	0.8729	2.2010	1.6554
	2	1.6400	3.7616	2.5672
	3	2.3130	3.7654	3.4642
	4	2.7100	5.6599	4.2174
	5	3.5488	5.9540	4.8091

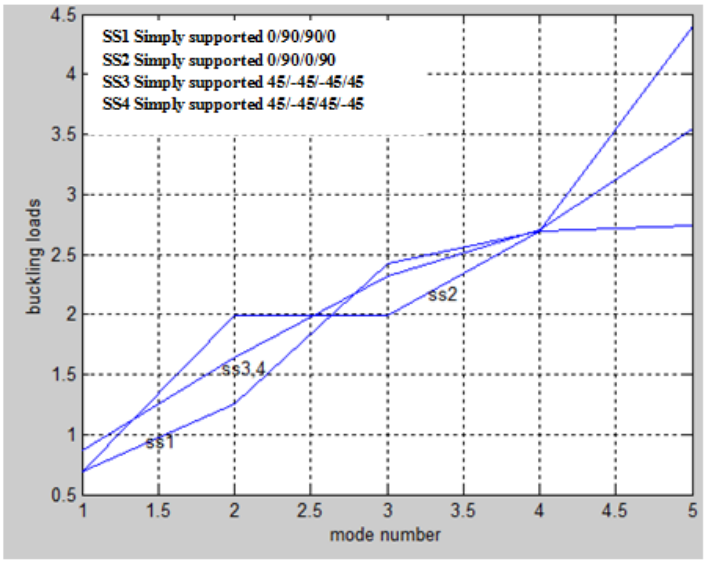

Figure 4. Effect of lamination scheme for simply supported laminates

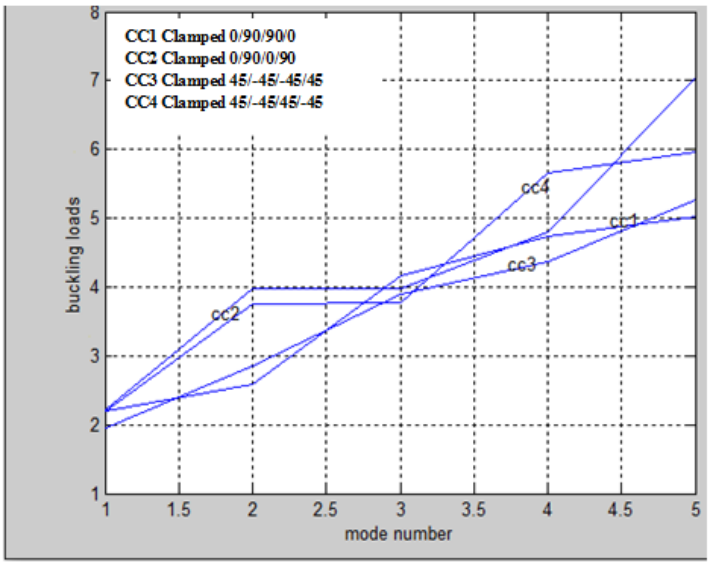

Figure 5. Effect of lamination scheme for clamped – clamped laminates

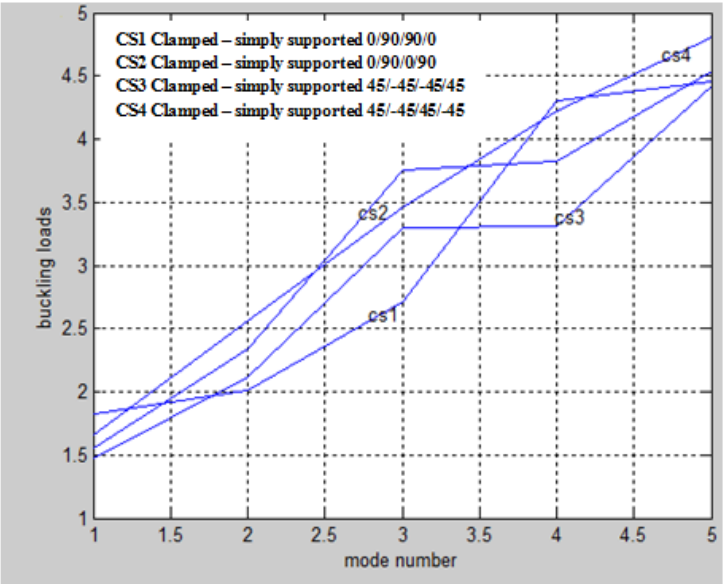

Figure 6. Effect of lamination scheme for clamped – simply supported laminates

Tables 4 and 5 show the buckling load of quasi – isotropic rectangular composite plate with $a/h = 20$, $a/b = 1$ and different modulus ratios ($E_1/E_2 = 40\ and\ 5$). The buckling load is highly influenced by its boundary conditions. The buckling load of the quasi – isotropic (0/+45/-45/90) rectangular composite plate with CC type boundary condition is 1.5 times higher than the buckling load of the composite plate with CS type boundary condition and more than 3 times of SS type boundary condition.

Table 4. The first three non – dimensional buckling loads of quasi – isotropic (0/+45/-45/90) laminated plates with a/h=20, and $E_1/E_2 = 40$

Mode Number	Boundary Conditions		
	SS	CC	CS
1	0.4905	1.6878	1.1683
2	1.4842	3.0187	1.7359
3	1.4850	3.0229	2.7673

Table 5. The first three non – dimensional buckling load of quasi – isotropic (0/+45/-45/90) laminated plates with a/h=20, and $E_1/E_2 = 5$

Mode Number	Boundary Conditions		
	SS	CC	CS
1	0.7338	2.2255	1.5717
2	2.0202	3.9506	2.3714
3	2.0214	3.9549	3.7214

4.2 Effect of aspect ratio

In this study, the buckling loads for symmetrically loaded laminated composite plates of layer orientation 0/90/90/0 have been determined for seven different aspect ratios ranging from 0.5 to 2.0 and two modulus ratios 40 and 5 as shown in tables 6 and 7 and figures 7 and 8. The first mode of buckling loads was considered. It is observed that the buckling load increases continuously with increasing aspect ratio but the rate of increase is not uniform. This may be due to the effect of bending – extensional twisting stiffness which increases the critical load. The buckling load is maximum for clamped – clamped (CC), clamped – simply supported (CS) while minimum for simply – simply supported (SS) boundary conditions. This means that as the plate becomes more restrained, its resistance to buckling increases. The reason is that the structural stiffness reduces due to its constrains.

Table 6. The first three non – dimensional buckling loads $\bar{P} = Pa^2/E_1h^3$ of symmetric cross – ply (0/ 90/ 90/ 0) laminated plates with $a/h = 20$, and $E_1/E_2 = 40$

Aspect Ratio ($\boldsymbol{a/b}$)	Mode Number	SS	CC	CS
0.5	1	0.4143	1.0742	0.9679
	2	0.4236	1.0941	1.0484
	3	0.5408	1.3751	1.1257
0.75	1	0.4300	1.2389	1.0444
	2	0.4978	1.2691	1.2043
	3	0.6520	1.8354	1.2921
1.0	1	0.4409	1.3795	1.0723
	2	0.5580	1.5286	1.3105
	3	1.0763	2.1648	1.6946
1.25	1	0.4224	1.5549	1.1349
	2	0.7795	1.7455	1.4327
	3	1.6164	3.0019	1.8042
1.5	1	0.4400	1.6402	1.2543
	2	1.0787	2.2999	1.3330
	3	1.6841	3.2702	2.4753
1.75	1	0.4885	1.8361	1.1494
	2	1.4473	3.0138	1.6342
	3	1.8520	3.6574	2.7310
2.0	1	0.5642	2.1358	1.1054
	2	1.7525	3.7696	2.0207
	3	1.8813	3.8703	2.8553

Table 7. The first three non – dimensional buckling loads $\bar{P} = Pa^2/E_1h^3$ of symmetric cross – ply (0/ 90/ 90/ 0) laminated plates with $a/h = 20$ and $E_1/E_2 = 5$

Aspect Ratio ($\boldsymbol{a/b}$)	Mode Number	Boundary Conditions		
		SS	CC	CS
0.5	1	0.6787	1.7786	1.6325
	2	0.6841	1.8364	1.7192
	3	0.8672	2.2141	1.9284
0.75	1	0.6698	2.0107	1.7117
	2	0.8831	2.1504	1.9339
	3	1.4912	2.7694	2.2689
1.0	1	0.6972	2.1994	1.8225
	2	1.2552	2.5842	2.0097
	3	2.4284	4.1609	2.7116
1.25	1	0.7726	2.3958	1.8397
	2	1.7753	3.5341	2.1821
	3	2.6844	5.1641	3.8539
1.5	1	0.8943	2.7961	1.7643
	2	2.4305	4.8034	2.7358
	3	2.6675	5.2420	4.6305
1.75	1	1.0588	3.3873	1.7741
	2	2.6919	5.4542	3.4532
	3	3.2171	6.3629	4.7373
2.0	1	1.2630	4.1517	1.8578
	2	2.7619	5.8342	4.3179
	3	4.1301	8.1942	4.6131

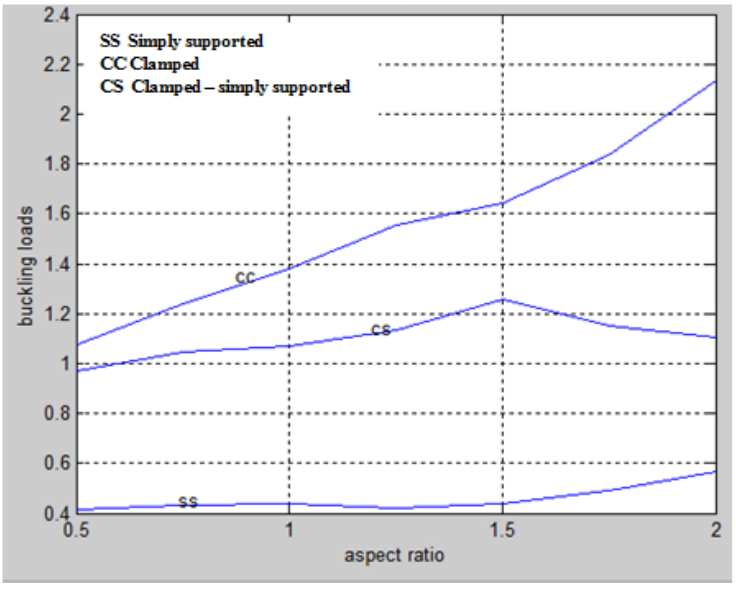

Figure 7. Effect of aspect ratio for different boundary conditions, $E_1/E_2 = 40$

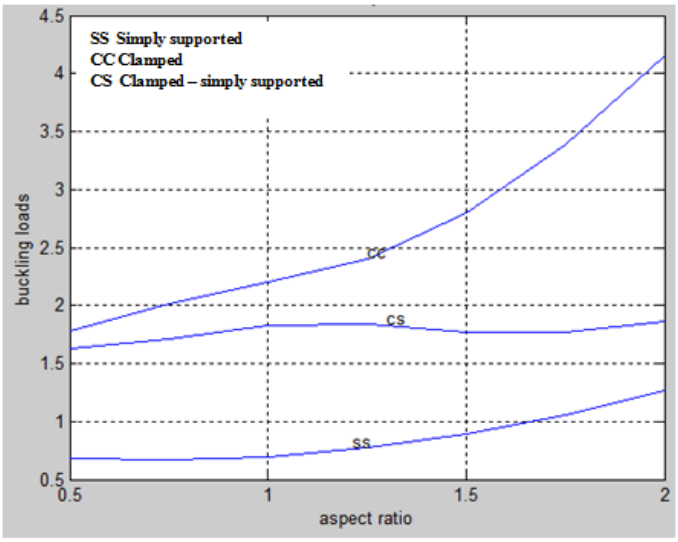

Figure 8. Effect of aspect ratio for different boundary conditions, $E_1/E_2 = 5$

4.3 Effect of material anisotropy

The buckling loads as a function of modulus ratio of symmetric cross – ply plates (0/ 90/ 90/ 0) are illustrated in table 8 and figure 9. As confirmed by other investigators, the buckling load decreases with increase in modulus ratio. Therefore, the coupling effect on buckling loads is more pronounced with the increasing degree of anisotropy. It is observed that the variation of buckling load becomes almost constant for higher values of elastic modulus ratio.

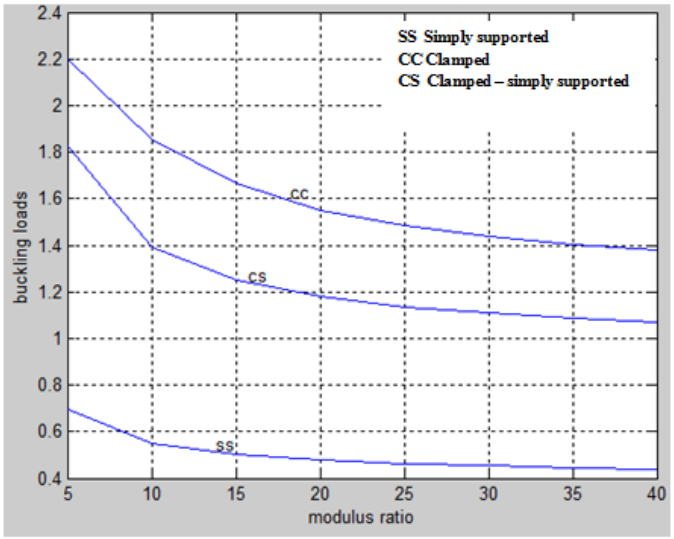

Figure 9. Effect of material anisotropy

Table 8. The first three non – dimensional buckling loads $\bar{P} = Pa^2/E_1h^3$ of symmetric cross – ply (0/ 90/ 90/ 0) square laminated plates for different modulus ratios with $a/h = 20$

E_1/E_2	Mode Number	Boundary Conditions		
		SS	CC	CS
5	1	0.6972	2.1994	1.8225
	2	1.2552	2.5842	2.0097
	3	2.4284	4.1609	2.7116
10	1	0.5505	1.8548	1.3928
	2	0.8557	1.8951	1.8292
	3	1.6532	2.9814	1.9089
15	1	0.5019	1.6663	1.2505
	2	0.7232	1.7248	1.6428
	3	1.3966	2.6049	1.7694
20	1	0.4775	1.5515	1.1791
	2	0.6569	1.6524	1.5096
	3	1.2683	2.4228	1.7394
25	1	0.4629	1.4828	1.1365
	2	0.6172	1.6055	1.4299
	3	1.1916	2.3171	1.7214
30	1	0.4531	1.4366	1.1078
	2	0.5907	1.5723	1.3766
	3	1.1402	2.2481	1.7094
35	1	0.4462	1.4044	1.0877
	2	0.5723	1.5479	1.3391
	3	1.1043	2.2006	1.7009
40	1	0.4409	1.3795	1.0723
	2	0.5580	1.5286	1.3105
	3	1.0763	2.1648	1.6946

4.4 Effect of fiber orientations of layers

The variation of the buckling load, $\bar{P}$ with fiber orientation (θ) of square laminated plate is shown in tables 9 and 10, and figures 10 and 11. Three boundary conditions SS, CC and CS are considered in this case. The buckling loads have been determined for two modulus ratios 40 and 5. The curves of simply – simply supported (SS) boundary conditions show maximum value of buckling load at $= 45^o$. However, this trend is different for a plate under clamped – clamed (CC) boundary conditions which show minimum buckling load at $\theta = 45^o$. For clamped – simply supported, it is observed that the buckling load decreases continuously with θ, this may be due to the total and partial fixed rotation ($\phi \; and \; \psi$) in the two later cases.

Table 9. The first three non – dimensional buckling loads $\bar{P} = Pa^2/E_1h^3$ of laminated plates for different fiber orientations (θ) with $a/h = 20$, and $E_1/E_2 = 40$

Orientation Angle (θ)	Mode Number	Boundary Conditions		
		SS	CC	CS
0	1	0.2604	0.6134	0.5561
	2	0.2825	0.6398	0.5729
	3	0.3960	0.8738	0.6745
15	1	0.2759	0.5957	0.5496
	2	0.3171	0.6123	0.5855
	3	0.4771	0.8638	0.7570
30	1	0.2823	0.5636	0.5114
	2	0.3125	0.5834	0.5352
	3	0.4861	0.9552	0.7902
45	1	0.2773	0.5207	0.4230
	2	0.3253	0.5842	0.4490
	3	0.5135	0.9793	0.7093
60	1	0.2834	0.5574	0.3073
	2	0.3116	0.5788	0.3895
	3	0.4783	0.9107	0.6362
75	1	0.2762	0.5859	0.3137
	2	0.3153	0.6043	0.3297
	3	0.4161	0.8252	0.4924
90	1	0.2602	0.6061	0.3069
	2	0.2811	0.6260	0.3438
	3	0.3908	0.8429	0.4801

Table 10. The first three non – dimensional buckling loads $\bar{P} = Pa^2/E_1h^3$ of laminated plates for different fiber orientations (θ) with $a/h = 20$, and $E_1/E_2 = 5$

Orientation Angle (θ)	Mode Number	Boundary Conditions		
		SS	CC	CS
0	1	0.6970	2.1130	1.6496
	2	1.0086	2.1396	2.0991
	3	1.7709	3.1397	2.1597
15	1	0.7108	2.0261	1.6665
	2	1.0908	2.1400	1.9833
	3	1.8704	3.2340	2.2141
30	1	0.7457	1.8142	1.6326
	2	1.2613	2.2494	1.7099
	3	2.0671	3.4809	2.4700
45	1	0.7665	1.7189	1.3114
	2	1.3477	2.3567	1.7689
	3	2.1557	3.5899	2.7032
60	1	0.7457	1.8147	1.0893
	2	1.2602	2.2457	1.7913
	3	2.0637	3.4650	2.6452

Orientation Angle (θ)	Mode Number	Boundary Conditions		
		SS	CC	CS
75	1	0.7110	2.0264	0.9824
	2	1.0898	2.1366	1.6562
	3	1.8659	3.2178	2.7338
90	1	0.6970	2.1101	0.9573
	2	1.0080	2.1389	1.5827
	3	1.7666	3.1269	2.7322

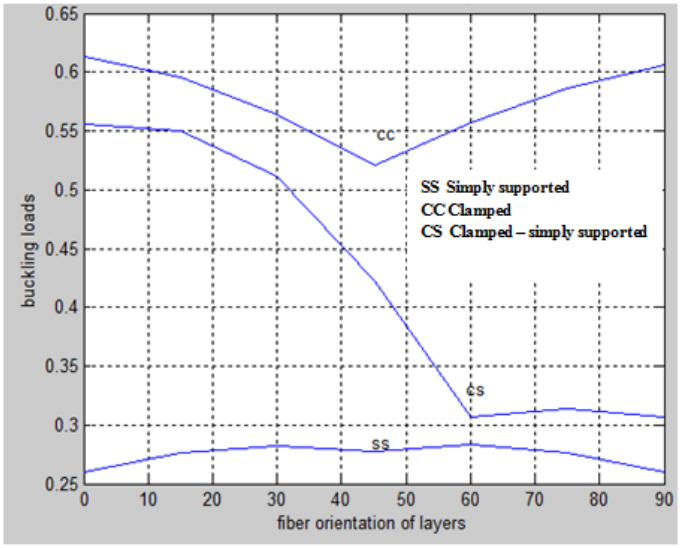

Figure 10. Effect of fiber orientation of layers, $E_1/E_2 = 40$

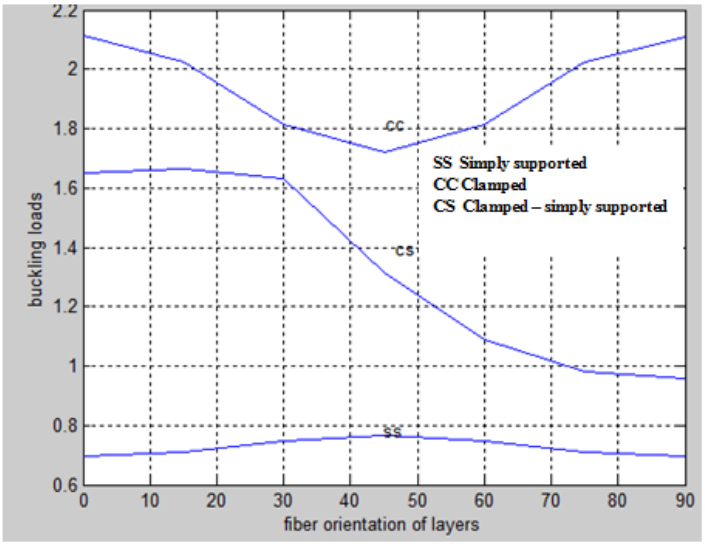

Figure 11. Effect of fiber orientation of layers, $E_1/E_2 = 5$

4.5 Effect of reversing lamination scheme

In order to study the stacking sequence of laminated plates, two lamination schemes of cross – ply (0/ 90) and (90/ 0) and two other lamination of angle ply (45/ -45) and (-45/ 45) were considered. The results of their buckling loads of parameter ($\bar{P} = Pa^2/E_1h^3$) are given in tables 11, 12, 13 and 14. Three boundary conditions SS, CC and CS are considered in this case. The buckling loads have been determined for two modulus ratios 40 and 5. It is observed that, the buckling loads are completely the same for the given first three modes.
Therefore, it can be concluded that the buckling load of laminated plates will remain the same even if the lamination order is reversed. The reason behind this is that the transformed elastic coefficients, $[C_{ij}]$, are equal for both lamination schemes.

Table 11. Non–dimensional buckling loads $\bar{P} = Pa^2/E_1h^3$ of (0/ 90) and (90/ 0) lamination schemes of square laminated plates with $a/h = 20$, and $E_1/E_2 = 40$

Lamination order	Mode Number	Boundary Conditions		
		SS	CC	CS
0/90	1	0.4410	1.6885	1.1512
	2	0.4494	3.0311	1.6881
	3	1.4502	3.0349	2.5982
90/0	1	0.4410	1.6885	1.1512
	2	0.4494	3.0311	1.6881
	3	1.4502	3.0349	2.5982

Table 12. Non–dimensional buckling loads $\bar{P} = Pa^2/E_1h^3$ of (0/ 90) and (90/ 0) lamination schemes of square laminated plates with $a/h = 20$, and $E_1/E_2 = 5$

Lamination order	Mode Number	Boundary Conditions		
		SS	CC	CS
0/90	1	0.6970	2.2275	1.5593
	2	1.9943	3.9687	2.3388
	3	1.9954	3.9733	3.7581
90/0	1	0.6970	2.2274	1.5594
	2	1.9944	3.9688	2.3393
	3	1.9957	3.9733	3.7580

Table 13. Non–dimensional buckling loads $\bar{P} = Pa^2/E_1h^3$ of (45/ -45) and (-45/ 45) lamination schemes of square laminated plates with $a/h = 20$, and $E_1/E_2 = 40$

Lamination order	Mode Number	Boundary Conditions		
		SS	CC	CS
45/-45	1	0.8375	1.6524	1.2806
	2	1.7263	2.7630	1.9965
	3	1.7285	2.7659	2.5358

-45/45	1	0.8372	1.6527	.2805
	2	.7262	2.7631	19963
	3	1.7283	2.7660	2.5355

Table 14. Non–dimensional buckling loads $\bar{P} = Pa^2/E_1h^3$ of (45/ -45) and (-45/ 45) lamination schemes of square laminated plates with $a/h = 20$, and $E_1/E_2 = 5$

Lamination order	Mode Number	Boundary Conditions		
		SS	CC	CS
45/-45	1	0.9907	2.2010	1.6553
	2	2.1995	3.7613	2.5668
	3	2.2015	3.7652	2.4640
-45/45	1	0.9908	2.2010	1.6553
	2	2.1995	3.7613	2.5671
	3	2.2015	3.7652	3.4636

4.6 Effect of boundary conditions

The type of boundary support is an important factor in determining the buckling loads of a plate along with other factors such as aspect ratio, modulus ratio, … etc.

Three sets of boundary conditions, namely simply – simply supported (SS), clamped – clamped (CC), and clamped – simply supported (CS) were considered in this study.

The variations of buckling load, $\bar{P}$ with the mode number for thin ($a/h = 20$) symmetrically loaded laminated cross – ply (0/90/90/0) plate with modulus ratio ($E_1/E_2 = 5$) were computed and the results are given in table 15 and figure 12.

It is observed that, for all cases the buckling load increases with the mode number but at different rates depending on whether the plate is simply supported, clamped or clamped – simply supported. The buckling load is a minimum when the plate is simply supported and a maximum when the plate is clamped. Because of the rigidity of clamped boundary condition, the buckling load is higher than in simply supported boundary condition. It is also observed that as the mode number increases, the plate needs additional support.

Table 15. The first five non–dimensional buckling loads $\bar{P} = Pa^2/E_1h^3$ of symmetric (0/90/90/0) square laminated plates with $a/h = 20$, and $E_1/E_2 = 5$

Mode Number	Boundary Conditions		
	SS	CC	CS
1	0.6972	2.1994	1.8225
2	1.2552	2.5842	2.0097
3	2.4284	4.1609	2.7116
4	2.6907	4.7431	4.3034
5	2.7346	5.0168	4.4536

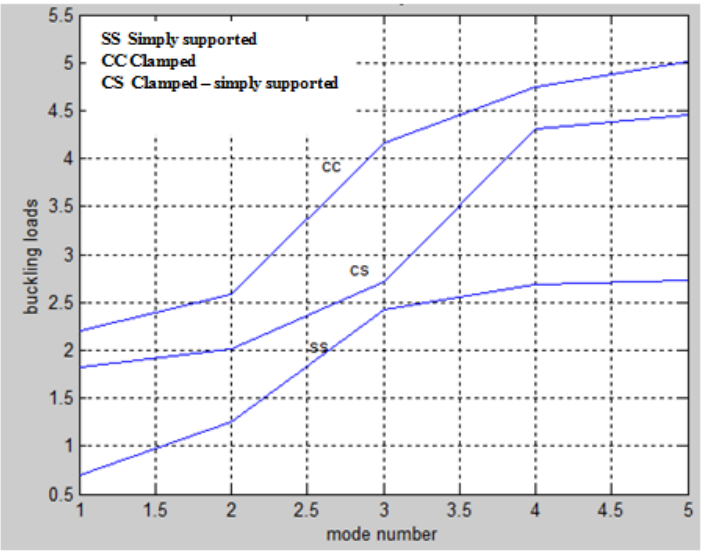

Figure 12. Effect of boundary conditions

5 CONCLUSIONS

A Fortran program based on finite elements (FE) has been developed for buckling analysis of thin rectangular laminated plates using classical laminated plate theory (CLPT). The problem of buckling loads of generally layered composite plates has been studied. The problem is analyzed and solved using the energy approach, which is formulated by a finite element model. In this method, quadrilateral elements are applied utilizing a four noded model. Each element has three degrees of freedom at each node. The degrees of freedom are: lateral displacement (w), and rotation (ϕ) and (ψ) about the x and y axes respectively. To verify the accuracy of the present technique, buckling loads are evaluated and validated with other works available in the literature. Further comparisons were carried out and compared with the results obtained by the ANSYS package and the experimental result. The good agreement with available data demonstrates the reliability of finite element method used.

The finite element model has been formulated to compute the buckling loads of laminated plates with rectangular cross – section and to study the effects of lamination scheme, aspect ratio, material anisotropy, fiber orientation of layers, reversed lamination scheme and boundary conditions on the non – dimensional critical buckling loads of laminated composite plates. Finally, a series of new results have been presented. These results show the following:

1. The symmetric laminate is stiffer than the anti – symmetric one. This phenomenon is caused by coupling between bending and stretching which lowers the buckling loads of symmetric laminate.
2. The buckling load is highly influenced by the end support. The buckling load

of the quasi – isotropic (0/+45/-45/90) rectangular composite plate with clamped – clamped type boundary condition is 1.5 times higher than the buckling load of the composite plate with clamped – simply supported (CS) type boundary condition, and more than 3 times of simply – simply supported (SS) type boundary condition.

3. The buckling load increases continuously with increasing aspect ratio, but the rate of increase is not uniform. This may be due to the effect of bending – extensional twisting stiffness which increases the critical load.
4. As the plate becomes more restrained, its resistance to buckling increases. The reason is that the structural stiffness reduces due to its constraints.
5. The buckling load decreases with increase in modulus ratio. It is also observed that the variation of buckling load becomes almost constant for higher values of elastic modulus. This may be attributed to the coupling effect which increases with the increasing degree of anisotropy.
6. The curves of simply – simply supported (SS) boundary conditions show maximum value of buckling load at $\theta = 45^o$. However, this trend is different for a plate under clamped – clamped (CC) boundary conditions which show minimum load at $\theta = 45^o$. For clamped – simply supported, it is observed that the buckling load decreases continuously with θ. This may be due to the total and partial fixed rotation ϕ and ψ in the two later cases.
7. The buckling load of laminated plates will remain the same even if the lamination order is reversed. The reason behind this is that the transformed elastic coefficients, $[C_{ij}]$, are equal for both lamination schemes.
8. The buckling load increases with the mode number but at different rates depending on whether the plate is simply supported (SS), clamped (CC) or clamped – simply supported. The buckling load is a minimum when the plate is simply supported and a maximum when the plate is clamped. Because of the rigidity of clamped boundary condition, the buckling load is higher than in simply supported boundary condition. It is also observed that as the mode number increases, the plate needs additional support.

ACKNOWLEDGMENTS

The authors would like to acknowledge with deep thanks and profound gratitude Mr. Osama Mahmoud of Daniya Center for Publishing and Printing Services, Atbara, who spent many hours in editing, re – editing of the manuscript in compliance with the standard format of International Journal of Bridge Engineering (IJBE) Journal.

REFERENCES

[1] David Roylance, 'An introduction to composite materials', Department of material science and engineering, Massachusetts Institute of Technology, Cambridge; (2000).

[2] Stephen W. Tsai, Thomas Hahn H., 'introduction to composite materials', Technomic

publishing company; (1980).
[3] Turvey G.J., Marshall I.H., 'buckling and post buckling of composite plates', Great Britain, T.J. press Ltd, Padstow, Cornwall; (1995).
[4] Mahmoud Yassin Osman and Osama Mohammed Elmardi Suleiman, ' Free Vibration Analysis of Laminated Composite Beams using Finite Element Method ', International Journal of Engineering Research and Advanced Technology (I JERAT), Volume 3, Issue 2; February (2017): PP. (5 – 22).
[5] Mahmoud Yassin Osman and Osama Mohammed Elmardi Suleiman, ' Free Vibration of Laminated Plates ', International Journal of Engineering Research and Advanced Technology (IJERAT), Volume 3, Issue 4; April (2017): PP. (31 – 47).
[6] Mahmoud Yassin Osman and Osama Mohammed Elmardi Suleiman, ' Large Deflection of Composite Beams ', International Journal of Engineering Research and Advanced Technology (IJERAT), Volume 3, Issue 3; March (2017): PP. (26 – 39).
[7] Osama Mohammed Elmardi Suleiman et al., ' Free Vibration Analysis of Composite Laminated Beams ', International Journal of Engineering Research and Advanced Technology (IJERAT), Volume 3, Issue 10; October (2017): PP. (31 – 47).
[8] Turvey G.J., Marshall I.H.,' Buckling and post buckling of composite plates', London: Chapman and Hall; (1995).
[9] Singer J., Arbocz J., Weller T.,' Buckling experiments: Experimental methods in buckling of thin walled strictures', vol.1, New York: John Willey and sons ;(1998).
[10] Singer J., Arbocz J., Wetter T.,' buckling experiments: Experimental methods in buckling of thin walled structures: shells, Built up structures, composites and additional topics', vol.2., New York: John Willey and Sons; (2002).
[11] Mahmoud Yassin Osman and Osama Mohammed Elmardi Suleiman, 'Buckling analysis of thin laminated composite plates using finite element method', International Journal of Engineering Research and Advanced Technology (I JERAT), Volume 3, Issue 3; March (2017): PP. (1 – 18).
[12] J. N. Reddy, 'Mechanics of laminated composite plates and shells, theory and analysis', second edition, CRC press, Washington; (2004).

APPENDICES

Appendix (A)

The transformed material properties are:

$$C_{11} = C'_{11}\cos^4\theta + C'_{22}\sin^4\theta + 2(C'_{12} + 2C'_{66})\sin^2\theta\cos^2\theta$$

$$C_{12} = (C'_{11} + C'_{22} - 4C'_{66})\sin^2\theta\cos^2\theta + C^1_{12}(\cos^4\theta + \sin^4\theta)$$

$$C_{22} = C'_{11}\sin^4\theta + C'_{22}\cos^4\theta + 2(C'_{12} + 2C'_{66})\sin^2\theta\cos^2\theta$$

$$C_{16} = (C'_{11} - C'_{12} - 2C'_{66})\cos^3\theta\sin\theta - (C'_{22} - C'_{12} - 2C'_{66})\sin^3\theta\cos\theta$$

$$C_{26} = (C'_{11} - C'_{12} - 2C'_{66})\cos\theta\sin^3\theta - (C'_{22} - C'_{12} - 2C'_{66})\sin\theta\cos^3\theta$$

$$C_{66} = (C'_{11} + C'_{22} - 2C'_{12} - 2C'_{66})\sin^2\theta\cos^2\theta + C'_{66}(\sin^4\theta + \cos^4\theta)$$

where $C'_{11} = \frac{E_1}{1 - \nu_{12}\nu_{21}}$, $C'_{22} = \frac{E_2}{1 - \nu_{12}\nu_{21}}$, $C'_{12} = \frac{\nu_{12}\, E_2}{1 - \nu_{12}\nu_{21}}$, $C'_{16} = G_{12}$

Appendix (B)

$a_{i,j}/8$

i / N_i	i.1	i,2	i,3	i,4	i,5	i,6	i,7	i,8	i,9	i,10	i,11	i,12
N_1	2	-3	3	0	-4	0	1	0	0	-1	1	1
N_2	1	-1	1	-1	-1	0	1	-1	0	0	1	0
N_3	-1	1	-1	0	1	1	0	0	-1	1	0	-1
N_4	2	-3	-3	0	4	0	1	0	0	1	-1	-1
N_5	1	-1	-1	-1	1	0	1	1	0	0	-1	0
N_6	1	-1	-1	0	1	-1	0	0	1	1	0	-1
N_7	2	3	3	0	4	0	-1	0	0	-1	-1	-1
N_8	-1	-1	-1	1	-1	0	1	1	0	0	1	0
N_9	-1	-1	-1	0	-1	1	0	0	1	1	0	1
N_{10}	2	3	-3	0	-4	0	-1	0	0	1	1	1
N_{11}	-1	-1	1	1	1	0	1	-1	0	0	-1	0
N_{12}	1	1	-1	0	-1	-1	0	0	-1	1	0	1

Appendix (C)

The integrals in equations (13) and (14) are given in nondimensional form as follows (limits of integration $r, s = -1$ to1):

$$\iint \frac{\partial^2 N_i}{\partial x^2}\frac{\partial^2 N_j}{\partial x^2}\,dx\,dy = \frac{4h_y}{h_x{}^3}\iint \frac{\partial^2 N_i}{\partial r^2}\frac{\partial^2 N_j}{\partial r^2}\,dr\,ds$$

$$= \frac{4n^3}{mR}\left(16a_{i,4}a_{j,4} + 48a_{i,7}a_{j,7} + 16a_{i,8}a_{j,8}/3 + 16a_{i,11}a_{j,11}\right)$$

$$\iint \frac{\partial^2 N_i}{\partial y^2}\frac{\partial^2 N_j}{\partial y^2}\,dx\,dy = \frac{4h_x}{h_y{}^3}\iint \frac{\partial^2 N_i}{\partial s^2}\frac{\partial^2 N_j}{\partial s^2}\,dr\,ds$$

$$= \frac{4m^3R^3}{n}\left(16a_{i,6}a_{j,6} + 16a_{i,9}a_{j,9}/3 + 48a_{i,10}a_{j,10} + 16a_{i,12}a_{j,12}\right)$$

$$\iint \frac{\partial^2 N_i}{\partial x^2}\frac{\partial^2 N_j}{\partial y^2}\,dx\,dy = \frac{4}{h_y h_x}\iint \frac{\partial^2 N_i}{\partial r^2}\frac{\partial^2 N_j}{\partial s^2}\,dr\,ds$$

$$= 4mnR\left(16a_{i,4}a_{j,6} + 16a_{i,7}a_{j,9} + 16a_{i,8}a_{j,10} + 16a_{i,11}a_{j,12}\right)$$

$$\iint \frac{\partial^2 N_i}{\partial y^2}\frac{\partial^2 N_j}{\partial x^2}\,dx\,dy = \frac{4}{h_y h_x}\iint \frac{\partial^2 N_i}{\partial s^2}\frac{\partial^2 N_j}{\partial r^2}\,dr\,ds$$

$$= 4mnR\left(16a_{i,6}a_{j,4} + 16a_{i,9}a_{j,7} + 16a_{i,10}a_{j,8} + 16a_{i,12}a_{j,11}\right)$$

$$\iint \frac{\partial^2 N_i}{\partial x\,\partial y}\frac{\partial^2 N_j}{\partial x\,\partial y}\,dx\,dy = \frac{4}{h_y h_x}\iint \frac{\partial^2 N_i}{\partial r\,\partial s}\frac{\partial^2 N_j}{\partial r\,\partial s}\,dr\,ds =$$

$$4mnR\left[4a_{i,5}a_{j,5} + 4(3a_{i,5}a_{j,11} + 4a_{i,8}a_{j,8})/3\right.$$

$$\left.+4(3a_{i,5}a_{j,12} + 4a_{i,9}a_{j,9})/3 + 4(a_{i,11}a_{j,12} + a_{i,12}a_{j,11}) + 36a_{i,12}a_{j,12}/5\right]$$

$$\iint \frac{\partial N_i}{\partial x}\frac{\partial N_j}{\partial x}\,dx\,dy = \frac{h_y}{h_x}\iint \frac{\partial N_i}{\partial r}\frac{\partial N_j}{\partial r}\,dr\,ds$$

$$= \frac{n}{mR}\big[4a_{i,2}a_{j,2} + 4(3a_{i,2}a_{j,7} + 4a_{i,4}a_{j,4} + 3a_{i,7}a_{j,2})/3$$

$$+4(a_{i,2}a_{j,9} + a_{i,5}a_{j,5} + a_{i,9}a_{j,2})/3 + 4(3a_{i,5}a_{j,11} + 3a_{i,7}a_{j,9} + 4a_{i,8}a_{j,8}$$

$$+3a_{i,9}a_{j,7} + 3a_{i,11}a_{j,5})/9 + 4(a_{i,5}a_{j,12} + a_{i,9}a_{j,9} + a_{i,12}a_{j,5})/5$$

$$+36a_{i,7}a_{j,7}/5 + 12a_{i,11}a_{j,11}/5 + 4(a_{i,11}a_{j,12} + a_{i,12}a_{j,11})/5 + 4a_{i,12}a_{j,12}/7\big]$$

$$\iint \frac{\partial N_i}{\partial y}\frac{\partial N_j}{\partial y}\,dx\,dy = \frac{h_x}{h_y}\iint \frac{\partial N_i}{\partial s}\frac{\partial N_j}{\partial s}\,dr\,ds$$

$$= \frac{mR}{n}\big[4a_{i,3}a_{j,3} + 4(a_{i,3}a_{j,8} + a_{i,5}a_{j,5} + a_{i,8}a_{j,3})/3$$

$$+4(3a_{i,3}a_{j,10} + 4a_{i,6}a_{j,6} + 3a_{i,10}a_{j,3})/3 + 4(3a_{i,5}a_{j,11} + a_{i,8}a_{j,8} + a_{i,11}a_{j,5})/5$$

$$+4(3a_{i,5}a_{j,12} + 3a_{i,8}a_{j,10} + 4a_{i,9}a_{j,9} + 3a_{i,10}a_{j,8} + 3a_{i,12}a_{j,5})/9$$

$$+36a_{i,10}a_{j,10}/5 + 4(a_{i,11}a_{j,12} + a_{i,12}a_{j,11})/5 + 12a_{i,12}a_{j,12}/5 + 4a_{i,11}a_{j,11}/7]$$

$$\iint \frac{\partial N_i}{\partial x}\frac{\partial N_j}{\partial y}\,dx\,dy = \iint \frac{\partial N_i}{\partial r}\frac{\partial N_j}{\partial s}\,dr\,ds$$

$$= 4a_{i,2}a_{j,3} + 4(a_{i,2}a_{j,8} + 2a_{i,4}a_{j,5} + 3a_{i,7}a_{j,8})/3 + 4(3\,a_{i,2}a_{j,10} + 2a_{i,5}a_{j,6}$$

$$+a_{i,9}a_{j,3})/3 + 4(2a_{i,4}a_{j,11} + 3a_{i,7}a_{j,8})/5 + 4(6a_{i,4}a_{j,12} + 9a_{i,7}a_{j,10}$$

$$+4a_{i,8}a_{j,9} + a_{i,9}a_{j,8} + 6a_{i,11}a_{j,6})/9 + 4(3a_{i,9}a_{j,10} + 2a_{i,12}a_{j,6})/5$$

$$\iint \frac{\partial N_i}{\partial y}\frac{\partial N_j}{\partial x}\,dx\,dy = \iint \frac{\partial N_i}{\partial s}\frac{\partial N_j}{\partial r}\,dr\,ds$$

$$= 4a_{i,3}a_{j,2} + 4(3a_{i,3}a_{j,7} + 2a_{i,5}a_{j,4} + a_{i,8}a_{j,2})/3 + 4(\,a_{i,3}a_{j,9} + 2a_{i,6}a_{j,5}$$

$$+3a_{i,10}a_{j,2})/3 + 4(6a_{i,6}a_{j,11} + a_{i,8}a_{j,9} + 4a_{i,9}a_{j,8} + 9a_{i,10}a_{j,7} + 6a_{i,2}a_{j,4})/9$$

$$+4(2a_{i,6}a_{j,12} + 3a_{i,10}a_{j,9})/5 + 4(3a_{i,8}a_{j,7} + 2a_{i,11}a_{j,4})/5$$

$$\iint \frac{\partial^2 N_i}{\partial x^2}\frac{\partial^2 N_j}{\partial x\,\partial y}\,dx\,dy = \frac{4}{h_x^{\,2}}\iint \frac{\partial^2 N_i}{\partial r^2}\frac{\partial^2 N_j}{\partial r\,\partial s}\,dr\,ds$$

$$= 4n^2\big[8a_{i,4}\big(a_{j,5} + a_{j,11} + a_{j,12}\big) + 16(a_{i,7}a_{j,8} + a_{i,8}a_{j,9}/3)\big]$$

$$\iint \frac{\partial^2 N_i}{\partial x\,\partial y}\frac{\partial^2 N_j}{\partial x^2}\,dx\,dy = \frac{4}{h_x^{\,2}}\iint \frac{\partial^2 N_i}{\partial r\,\partial s}\frac{\partial^2 N_j}{\partial r^2}\,dr\,ds$$

$$= 4n^2\big[8a_{j,4}\big(a_{i,5} + a_{i,11} + a_{i,12}\big) + 16a_{i,8}a_{j,7} + 16a_{i,9}a_{j,8}/3\big]$$

$$\iint \frac{\partial^2 N_i}{\partial y^2}\frac{\partial^2 N_j}{\partial x\,\partial y}\,dx\,dy = \frac{4}{h_y^{\,2}}\iint \frac{\partial^2 N_i}{\partial s^2}\frac{\partial^2 N_j}{\partial r\,\partial s}\,dr\,ds$$

$$= 4m^2R^2\big[8a_{i,6}\big(a_{j,5} + a_{j,11} + a_{j,12}\big) + 16a_{i,10}a_{j,9} + 16a_{i,9}a_{j,8}/3\big]$$

$$\iint \frac{\partial^2 N_i}{\partial x\,\partial y}\frac{\partial^2 N_j}{\partial y^2}\,dx\,dy = \frac{4}{{h_y}^2}\iint \frac{\partial^2 N_i}{\partial r\,\partial s}\frac{\partial^2 N_j}{\partial s^2}\,dr\,ds$$

$$= 4m^2R^2\left[8a_{j,6}\left(a_{i,5} + a_{i,11} + a_{i,12}\right) + 16a_{i,9}a_{j,10} + 16a_{i,8}a_{j,9}/3\right]$$

In the above expressions $h_x = \frac{a}{n}$, $h_y = \frac{b}{m}$ where a and b are the dimensions of the plate in the x – and y – directions respectively. n and m are the number of elements in the x – and y – directions respectively. Note that $dx = \frac{h_x}{2}dr$ and $dy = \frac{h_y}{2}ds$ where r and s are the normalized coordinates, and $R = a/b$.